Rekayasa Hijau: Jurnal Teknologi Ramah Lingkungan Volume 10 | Nomor 1
ISSN [e]: 2579-4264 | DOI: https://doi.org/10.26760/jrh.V10i1.1-11 Maret 2026

Kinetic Modeling of Ni and Co Adsorption: A Comparative Study on Activated Zeolite

Fikrah Dian Indrawati Sawali[1], Moh. Azhar Afandy[2]
[1,2]Mineral Chemical Engineering, Politeknik Industri Logam Morowali, Morowali, 94974, Indonesia

Email:fikrah@pilm.ac.id, azhar@pilm.ac.id[1]

3 Januari 2026 | Revised 15 Januari 2026 | Accepted 20 Januari 2026

ABSTRAK

Kehadiran logam berat seperti nikel (Ni) dan kobalt (Co) dalam air limbah berpotensi menyebabkan dampak lingkungan yang signifikan, sehingga diperlukan metode pengolahan yang efisien. Studi ini mengevaluasi kinetika adsorpsi Ni dan Co menggunakan zeolit alam yang diaktivasi secara termal melalui kalsinasi pada suhu 550°C. Proses adsorpsi dilakukan dengan variasi rasio massa adsorben dan dianalisis menggunakan beberapa model kinetika, yaitu Pseudo-First-Order (PFO), Pseudo-Second-Order (PSO), Intra-Particle Diffusion (IPD), dan Liquid Film Diffusion (LFD). Hasil penelitian menunjukkan bahwa proses adsorpsi Ni dan Co paling sesuai dengan model kinetika PSO, dengan koefisien determinasi (r^2) lebih dari 0,99. Kapasitas adsorpsi kesetimbangan yang diperoleh mencapai 9,4877 mg g^{-1} untuk Ni dan 7,3206 mg g^{-1} untuk Co. Temuan ini menunjukkan bahwa proses adsorpsi dikendalikan oleh interaksi kimia melalui mekanisme pertukaran ion pada permukaan zeolit.

***Kata kunci**: Adsorpsi, Nikel, Kobalt, Zeolit*

ABSTRACT

The presence of heavy metals such as nickel (Ni) and cobalt (Co), in wastewater poses significant environmental risks, necessitating the development of efficient treatment methods. This study investigates the adsorption kinetics of Ni and Co using natural zeolite thermally activated by calcination at 550°C. Adsorption experiments were conducted with varying adsorbent mass ratios and analysed using several kinetic models: Pseudo-First-Order (PFO), Pseudo-Second-Order (PSO), Intra-Particle Diffusion (IPD), and Liquid Film Diffusion (LFD). The results demonstrate that the adsorption of Ni and Co is best described by the PSO kinetic model, with a coefficient of determination (r^2) exceeding 0.99. The equilibrium adsorption capacities achieved were 9.4877 mg g^{-1} for Ni and 7.3206 mg g^{-1} for Co. These findings suggest that adsorption is governed by chemical interactions via ion-exchange mechanisms at the zeolite surface.

***Keywords**: Adsorption, Nickel, Cobalt, Zeolite*

1. INTRODUCTION

The removal of heavy metal ions from wastewater represents a significant environmental challenge due to their toxicity and persistence [1] . Nickel and cobalt, commonly found in industrial wastewater, pose significant health risks if not properly managed. These metals, which exist as divalent ions, are widely utilized in industries such as electroplating, tanning, oil refining, and electric battery manufacturing [1]–[4]. The rapid growth of the electric battery sector is expected to increase pollution from nickel and cobalt, both of which are essential raw materials. Contamination can occur during extraction, purification, or waste-disposal processes, leading to the accumulation of these metals in aquatic systems and harming microorganisms and aquatic organisms [5]. Furthermore, direct exposure to elevated concentrations of nickel and cobalt can negatively impact human health, resulting in skin irritation, respiratory problems, immune disorders, and damage to internal organs such as the kidneys, lungs, and thyroid gland [5]–[8]

Several techniques are available for the removal of nickel and cobalt, including adsorption, bioremediation, membrane technology, flotation, and electrocoagulation [9]–[12]. Conventional methods such as chemical precipitation and membrane processes often involve complex operations, high energy requirements, and the generation of secondary sludge. In comparison, adsorption has attracted considerable attention due to its lower cost, operational simplicity, broad availability of adsorbents, and environmental sustainability [13]–[17]. Previous studies have demonstrated that adsorption is highly efficient for the removal of nickel and cobalt, with systems capable of removing 80–90% of Ni(II) and Co(II) ions under optimized conditions [12], [18]. Natural zeolite is a widely used adsorbent for heavy metal removal, offering advantages such as a uniform micropore structure, high ion exchange capacity, chemical and thermal stability, cost-effectiveness, and regenerability [19], [20]. Natural zeolites are crystalline microporous aluminosilicate minerals characterized by a framework structure and composed of components such as silica (SiO_2), alumina (Al_2O_3), metal ions (Na^+, K^+, Ca^{2+}, Mg^{2+}), and water [21], [22]. In the present study, commercial natural zeolite sourced from a local marketplace was used as the raw material and subsequently activated through thermal treatment to improve its adsorption performance.

While numerous studies have explored heavy metal removal using various adsorbents, relatively few have investigated the adsorption of Ni(II) and Co(II) on thermally activated natural zeolite. Most existing research has focused on adsorption efficiency or equilibrium, with limited attention to kinetic aspects, specifically changes in adsorption rate over time. The mechanisms governing adsorption, including surface reactions and diffusion processes, remain insufficiently understood. Improved knowledge of these kinetic mechanisms is essential for optimizing the removal of heavy metals from aqueous solutions. Accordingly, this study examines the adsorption kinetics of Ni(II) and Co(II) ions using thermally activated natural zeolite. Several kinetic models—pseudo-first-order (PFO, which assumes the adsorption rate is proportional to the number of unoccupied sites), pseudo-second-order (PSO, which assumes chemisorption as the rate-limiting step), intra-particle diffusion (IPD, which considers ion movement within adsorbent particles), and liquid film diffusion (LFD, which considers resistance due to a boundary layer around the adsorbent)—are employed to evaluate adsorption behavior and identify the controlling mechanisms.

2. METHODOLOGY

2.1 Materials

This study utilizes Commercial natural zeolite from a local marketplace, Nickel chloride hexahydrate ($NiCl_2 \cdot 6H_2O$), Cobalt chloride hexahydrate ($CoCl_2 \cdot 6H_2O$), Dimethylglyoxime, Ammonium persulfate ($NH_4S_2O_8$), Ammonium hydroxide 25% (NH_4OH), Hydrochloric acid 37% (HCl), Ammonium thiocyanate (NH_4SCN), Acetone (C_3H_6O), Filter paper, and Distilled water from local suppliers. Each material considered in this inquiry have standard analytical requirements with a purity of 99%. This experiment utilized Erlenmeyer flasks, measuring flasks, beakers, funnels, 100 mesh sieves, Cryste-Puriven ovens (South Korea), and Naber Therm B-180 furnaces (Germany).

2.2 Activated Zeolite Preparation

Natural zeolite was sourced from a commercial supplier on an online marketplace in Bandung, Indonesia. The material consisted of light gray granular particles. Activated zeolite was produced via thermal activation according to established procedures [20]. The zeolite was ground in a laboratory mortar and pestle to reduce particle size, then sieved to obtain particles approximately 100 mesh. The sieved zeolite was dried in an oven at 110°C for 6 hours to eliminate moisture. The dried material was subsequently calcined at 550°C for 4 hours in a muffle furnace (Naber Therm B-180). The final product was designated as activated zeolite (ZT).

2.3 Batch Adsorption

Adsorption experiments for Ni and Co were performed in batch mode using 250 mL Erlenmeyer flasks maintained at room temperature (±28°C). Activated zeolite (ZT) was added to each flask, with adsorbent masses ranging from 0.5 to 2 g. Artificial wastewater containing Ni (100 mg L^{-1}) and Co (100 mg L^{-1}) was prepared by dissolving $NiCl_2 \cdot 6H_2O$ (0.4050 g) and $CoCl_2 \cdot 6H_2O$ (0.4040 g) separately in 1 L volumetric flasks, followed by dilution with distilled water. Adsorption experiments were conducted over contact times ranging from 30 to 180 minutes, consistent with previous studies. After the adsorption process, the solution was filtered, and the remaining metal concentrations were analyzed using a visible spectrophotometer (ICEN IN-B046, China) at 445 nm for Ni and 625 nm for Co, according to the method described by Sirotiak et al. [23]. The adsorption capacities of Ni and Co were calculated using Equation (1).

$$q_t = \frac{(C_O\text{-}C_t)\times V}{m} \quad (1)$$

Where the qt value is the adsorption capacity at t, Co is the initial Ni and Co concentration (mg. L^{-1}), Ct is the Ni and Co concentration at t, V is the initial Ni and Co volume (L), and m is the mass of the adsorbent (g).

2.4 Kinetics Model

Pseudo-first-order (PFO) and pseudo-second order (PSO) kinetic models were used to evaluate the kinetic parameters of Ni and Co adsorption onto the ZT adsorbent. Kinetic analyses were performed to elucidate the adsorption rates and underlying mechanisms. Additionally, intra-particle diffusion (IPD) and liquid film diffusion (LFD) models were used to investigate the mechanisms that affect adsorption. The equations corresponding to the kinetic models used in this study are provided in Table 1.

Table 1 Kinetic Models of Adsorption

Kinetics Model	Equation
Pseudo-First-Order	$log(q_e - q_t) = log\, q_e - \frac{k_1}{2.303} t$
Pseudo-Second-Order	$\frac{t}{q_t} = \frac{1}{k_2 {q_e}^2} + \frac{t}{q_e}$
Intra Particle Diffusion	$q_t = K_{int} t^{1/2} + C$
Liquid Film Diffusion	$\ln\left(1 - \frac{q_t}{q_e}\right) = -Kt$

Where, qe is the adsorption capacity, qt is the adsorption capacity at time (t), while the values k_1 & k_2 indicate the order of each kinetic model, and K_{int} is the constant of intra-particle diffusion. Thecorrelation coefficient (R^2) is used as a reference to assess the acceptability of the kinetic model derived from experimental data on the adsorption of Ni and Co by ZT. The R^2 value can indicate how well the kinetic model fits the relationship between time and the amount of adsorbate (Ni and Co) on the ZT surface. The appropriateness of the kinetic model will be considered a good fit when the R^2 value is > 0.95 or approaches 1.

3. RESULTS AND DISCUSSION

3.1 Effect of Activated Zeolite Mass

The mass of the adsorbent in this situation, ZT, is one of the main variables in influencing the efficiency and adsorption capacity acquired from the work of the adsorbent. Thus, the mass of the adsorbent is one of the quite significant parameters. In this work, the mass of ZT utilized varied from 0.5 to 2 g for the adsorption process of Ni and Co. The adsorption capacity values of the ZT adsorbent against Ni and Co can be seen in Figures 1a and 1b.

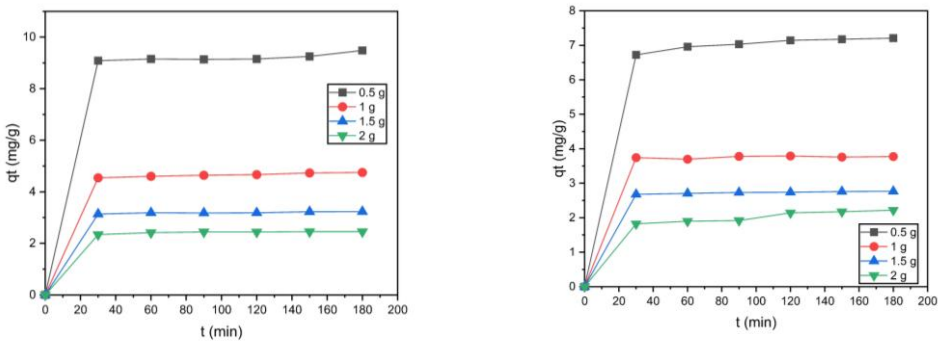

(a) (b)

Figure 1 Effect of ZT mass for (a) Ni and (b) Co adsorption capacity

Based on the data obtained in Figures 1a and 1b, the mass of ZT has a significant effect on the adsorption capacity of Ni and Co. In general, a larger adsorbent mass tends to reach adsorption equilibrium more quickly. In contrast, at a lower adsorbent mass (0.5 g), the adsorption capacity (qt) still increases with time, indicating that equilibrium had not been fully achieved within the observed time range. The adsorption process generally occurs more rapidly during the initial stage of the experiment. However, since the first sample was taken at 30 minutes, the rapid adsorption phase that may have occurred before this time could not be clearly observed. In addition, a smaller ZT mass tends to produce a higher adsorption capacity per gram of adsorbent. This occurs because, at lower adsorbent mass, the number of metal ions (Ni and Co) in solution is relatively higher compared to the available adsorption sites, leading to greater competition among ions to occupy the active sites. Conversely, at higher adsorbent

mass, the available active sites increase while the concentration of metal ions remains constant, resulting in lower adsorption capacity per gram of adsorbent. This trend is consistent with previous studies reported by Kushwaha, Rasheed, and Tuesta [18], [24], [25]. focusing on the influence of mass on the adsorption capacity of Ni and Co.

Figures 1a and 1b indicate that the adsorption capacities of Ni and Co increase substantially during the first 30 minutes, followed by a slower increase until equilibrium is achieved. The initial sampling time in this study was set at 30 minutes based on experimental constraints and preliminary observations. Consequently, any rapid adsorption phase occurring before 30 minutes was not captured in the current dataset. This is because there are still numerous active sites available at the first stage of adsorption on the ZT surface and the presence of a very strong concentration gradient. Which will subsequently slow down due to the competition between ions that happens and the reduction in active sites accessible on the ZT surface. In the last stage, the adsorption process of Ni and Co will normally be controlled by the intraparticle diffusion mechanism until the system reaches adsorption equilibrium. When compared, the adsorption capacity value of ZT for Ni tends to be larger than Co, which can be seen in Figures 1a and 1b and attached in Tables 1 and 2. This can be influenced by numerous aspects, including Ni having a smaller ionic radius (0.69 Å) as compared to Co (0.72 Å), Zeolites typically possess pore sizes ranging from 3 to 10 Å (0.3–1.0 nm) and feature an aluminosilicate crystal framework. The specific pore size is determined by the characteristics of this crystal framework [26]. Hence Ni has a tendency to permeate more easily into the pores of the ZT adsorbent and subsequently will interact with the accessible active sites. Hydration energy also plays an essential function, as the hydration energy value will reflect how strongly the ion interacts with water molecules in the solution. More negative hydration energy will tend to be stable in solution but also show a higher tendency to interact with active sites on the adsorbent if the interaction force is supportive. Because the hydration energy of Ni is slightly lower than Co, Ni tends to be more adsorbed on the negatively charged adsorbent surface. Theoretical calculations indicate that the hydration energy of Ni and Co ranges from −2105 kJ mol^{-1} to −2056 kJ mol^{-1} [27]. Zeolites usually have high ion exchange capacity, which implies they are able to exchange metal ions with ions in their structure. Because Ni has a higher affinity for ion exchange sites in zeolites than Co, the amount of Ni adsorbed is usually greater. Nickel (Ni) exhibits a higher affinity for ion exchange at the surface due to its ions being slightly smaller than those of cobalt (Co). Smaller ions generally possess stronger electrostatic affinity and higher charge density [28]. Several studies have demonstrated that zeolites are more likely to adsorb Ni than Co due to the difference in cation affinity for active sites in zeolites [21], [29], [30].

3.2 Adsorption Kinetics

The adsorption kinetics in this study have been investigated using the PFO and PSO kinetic models, and the processes that influence the adsorption of Ni and Co on ZT adsorbent were evaluated using the IPD and LFD kinetic models. The plotting results of the PSO and PFO kinetic models can be seen in Figures 2a and 2b and Figures 3a and 3b, while the parameter values obtained can be seen in Tables 1 and 2.

The PFO kinetic model assumes that external diffusion handles the adsorption process that happens, and the rate of the adsorption process will be proportional to the number of active sites that are still available on the adsorbent surface. The PFO model also shows that there is no interaction between adsorbate molecules after binding to the adsorbent surface. The results obtained based on the PFO model may be observed in Figures 2a and 2b by graphing t vs log (qe-qt). Based on the parameter data of the PFO kinetic model for the adsorption process of Ni and Co which can be seen in Tables 1 and 2, the maximum adsorption capacity value (qe) for Ni and Co on the ZT adsorbent surface tends to increase with increasing adsorbent mass for Ni and the qe value tends to fluctuate for Co. The qe values obtained for Ni and Co have quite a substantial discrepancy when compared to the qe values obtained in the experimental data. This reveals that the adsorption process of Ni and Co by the ZT adsorbent does not

have a good level of compatibility if expected according to the PFO kinetic model. The observed increase in qe value for PFO with greater adsorbent mass results from a higher number of active sites on the adsorbent surface, which facilitates increased interaction with metal ions.

The contrary is indicated by the PSO kinetic model. The PSO kinetic model itself presupposes that the adsorption rate will be regulated by chemical interactions, not merely through external diffusion. In this situation, the adsorption process of Ni and Co by ZT adsorbent can occur by ion exchange or through the creation of covalent bonds between Ni or Co and ZT adsorbent. The results of plotting t vs. t/qt from the PSO kinetic model can be observed in Figures 2c and 2d. Based on the parameter data of the PSO kinetic model, which can be shown in Tables 1 and 2, the qe value obtained tends to be near to the qe value obtained based on experimental data, thus confirming the appropriateness of the PSO model with experimental data. The qe value produced based on the PSO kinetic model similarly indicates a reduction along with the rising mass of the adsorbent, which is in accordance with the reasons mentioned previously in this study. In addition, one of the parameters that plays a significant role in the PSO kinetic model is the k_2 value (PSO kinetic rate constant). Based on the data provided in Tables 1 and 2, the k_2 value for the adsorption of Ni and Co will exhibit a decrease along with the increase in the mass of the ZT adsorbent. This can be influenced by the decrease in the concentration of Ni and Co metal ions, where more metal ions are adsorbed at the beginning of the process so that the ion concentration in the solution drops more rapidly with increasing mass. In addition, at a lower ZT adsorbent mass, practically all active sites are available to interact with Ni and Co ions, so that the adsorption process takes place quickly. Also, when the ZT adsorbent mass grows, the adsorbent particles tend to agglomerate due to interparticle interactions, reducing the effective specific surface area and creating reduced accessibility of active sites, hence slowing down the adsorption process of Ni and Co. The applicability of the PSO model can also be proved through the R^2 value > 0.99. So it can be concluded that the adsorption of Ni and Co by the ZT adsorbent follows the PSO kinetic model and is controlled by chemical interactions.

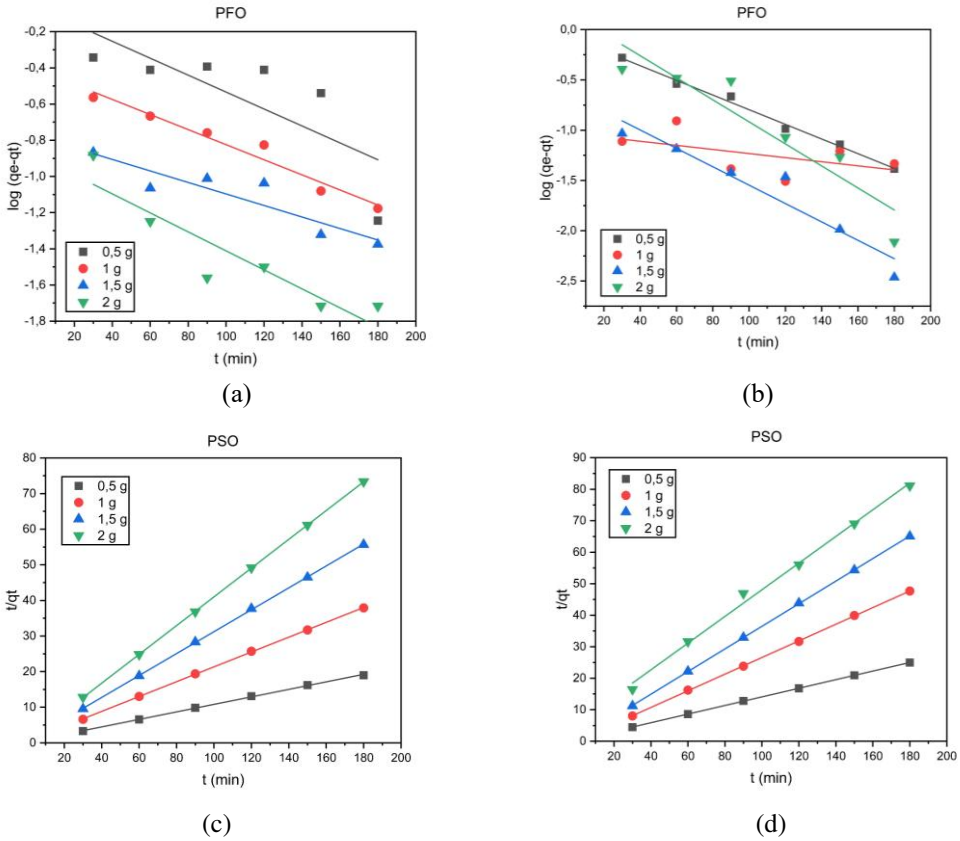

Figure 2 Linear regression of PFO kinetics models (a) Ni , (b) Co, and PSO kinetics models (c) Ni, (d) Co

Based on various earlier research by [22], [31]–[33], it was suggested that zeolite will have a pore structure with a negative charge due to the presence of Si-O- and Al-O- groups in the form of aluminosilicate. Ni and Co metal ions in solution can replace weaker ions such as Na, K, or Ca in the zeolite structure through an ion exchange mechanism. The results of prior investigations also demonstrated that zeolite contains hydroxyl groups (-OH), Si-OH, and Al-OH, which can interact with Ni and Co through coordinate covalent bonds. So that the PSO kinetic model will be proven through ion exchange processes and complex creation through coordinate covalent bonds.

The adsorption mechanism of Ni and Co can occur through numerous steps. First, the Ni and Co metal ions in the solution will travel towards the surface through the diffusion stage through external diffusion and then will be attracted through electrostatic forces. The process of ion exchange and complexation with functional groups will then occur. After all Ni and Co ions are adsorbed on the surface, they will next undergo an intraparticle diffusion process inside the ZT pore structure and reach equilibrium. The transopt mechanism that happens in the adsorption of Ni and Co can be analyzed using the IPD and LFD kinetic models. The IPD kinetic model can explain the diffusion of Ni and Co ions into the pores of ZT, where the IPD model posits that diffusion in the pores is the stage that governs adsorption. The IPD kinetic model also proposes that adsorption can occur in three stages, namely, liquid film diffusion (external diffusion), intraparticle diffusion, and equilibrium. The plotting results of the IPD kinetic model using t1/2 vs. qt values can be observed in Figures 3a and 3b.

Based on the IPD kinetic model parameter data that can be seen in Tables 1 and 2, there are two parameters that are utilized as references in the IPD kinetic model, namely the Kint and C values. The Kint value has quite an influence on the Ni adsorption process with a value that decreases with the ZT mass but gives a value that tends to fluctuate for the Co adsorption process. The decrease in the Kint value related to the intraparticle diffusion constant can be influenced by more Ni and Co ions, which can be caused by Ni and Co ions that tend to be more adsorbed on the ZT surface so that the active sites on the ZT surface are sufficient to adsorb most of the Ni and Co metal ions. Thus, that intraparticle diffusion is not a determinant in influencing the Ni and Co adsorption process by the ZT adsorbent. At a larger adsorbent mass, the adsorbent particles will also begin to agglomerate such that the contact area with the solution will decrease. A similar thing is also illustrated by the C value related to the thickness of the liquid film diffusion boundary layer, where there is a drop in the C value along with the growing adsorbent mass. The decrease can be caused by several factors where, when the mass of the adsorbent is greater, it will cause a higher concentration gradient between the solution and the surface of the adsorbent, causing the metal ions to move faster, resulting in a reduced thickness of the diffusion boundary layer because the metal ions are easier to pass through this zone to the surface of the adsorbent. When the bulk of the adsorbent is tiny, the number of active sites is limited, thus the metal ions have to wait longer before they can connect to the surface of the adsorbent.

In addition, the LFD kinetic model is also employed to investigate the adsorption mechanism of Ni and Co by ZT adsorbent. The LFD kinetic model posits that the passage of adsorbate molecules through the liquid layer around the solid adsorbent is the slowest phase in the adsorption process. The plotting results of the t vs. -ln(1-(qt/qe)) values are used for the LFD kinetic model and can be seen in Figures 3c and 3d. Important parameters in the LFD kinetic model are the Kfd and t1/2 values and may be observed in Tables 1 and 2. According to the data obtained for the adsorption process of Ni and Co by ZT according to the LFD kinetic model on the mass comparison of the adsorbent, the Kfd value on the adsorption of Ni and Co is very fluctuating so that it can be said that the LFD kinetic model is not suitable for use in the adsorption process of Ni and Co by ZT adsorbent. The Kfd value itself affects the value of the liquid film diffusion constant. The R^2 value of the IPD and LFD kinetic models displays a value that is not

satisfactory when compared to the PSO kinetic model. Consequently, it can be concluded that the film layer diffusion model and intra-particle diffusion do not represent the adsorption stages of Ni and Co by zeolite but likely only play a role in the initial stages of adsorption, which will then be dominated by chemical interactions through ion exchange and the formation of coordinate covalent bonds, which will then form complex compounds with active sites on the surface of the ZT adsorbent. Experimental uncertainty is anticipated to be minimal, as all experiments were conducted under consistent procedures and controlled conditions.

Table 1 Kinetics parameter of Ni

Kinetics Models	ZT mass (g)			
	0,5	1	1,5	2
Pseudo-first-order (PFO)				
qe ($mg.g^{-1}$)	1,0679	1,5031	2,1782	2,4261
k_1 (min^{-1})	0,0108	0,0096	0,0074	0,0122
R^2	0,5859	0,9617	0,8332	0,8375
Pseudo-second-order (PSO)				
qe ($mg.g^{-1}$)	9,4877	4,8008	3,2510	2,4759
k_2 ($g.mg^{-1}.min^{-1}$)	329,6075	44,7348	22,8812	9,9705
R^2	0,9991	0,9999	0,9999	0,9999
Intra-particle diffusion (IPD)				
K_{int} ($mg.\ g^{-1}\ min^{-1/2}$)	0,0392	0,0265	0,0107	0,0130
C ($mg.g^{-1}$)	8,8206	4,3936	3,8050	2,2966
R^2	0,6418	0,9825	0,8274	0,7856
Liquid film diffusion (LFD)				
K_{fd} (min^{-1})	0,0108	0,0096	0,0073	0,0121
$t_{1/2}$ (s)	64,1677	72,1875	94,9315	57,2727
R^2	0,5859	0,9617	0,8332	0,8375

Table 2 Kinetics parameter of Co

Kinetics Models	ZT mass (g)			
	0,5	1	1,5	2
Pseudo-first-order (PFO)				
qe ($mg.g^{-1}$)	1,0695	2,7980	1,8816	1,1958
k_1 (min^{-1})	0,0168	0,0046	0,0209	0,0253
R^2	0,9916	0,2330	0,9151	0,8375
Pseudo-second-order (PSO)				
qe ($mg.g^{-1}$)	7,3206	3,7864	2,7871	2,3618
k_2 ($g.mg^{-1}.min^{-1}$)	127,9652	89,6633	13,0222	0,9713
R^2	0,9999	0,9999	0,9999	0,9948
Intra-particle diffusion (IPD)				
K_{int} ($mg.\ g^{-1}\ min^{-1/2}$)				
C ($mg.g^{-1}$)	0,0599	0,0065	0,0113	0,0547
R^2	6,4479	3,6927	2,6174	1,4881
	0,9449	0,3190	0,9800	0,9113
Liquid film diffusion (LFD)				
K_{fd} (min^{-1})	0,0168	0,0047	0,0211	0,0252
$t_{1/2}$ (s)	41,2500	147,4468	32,8436	27,5000
R^2	0,9916	0,2833	0,9151	0,8661

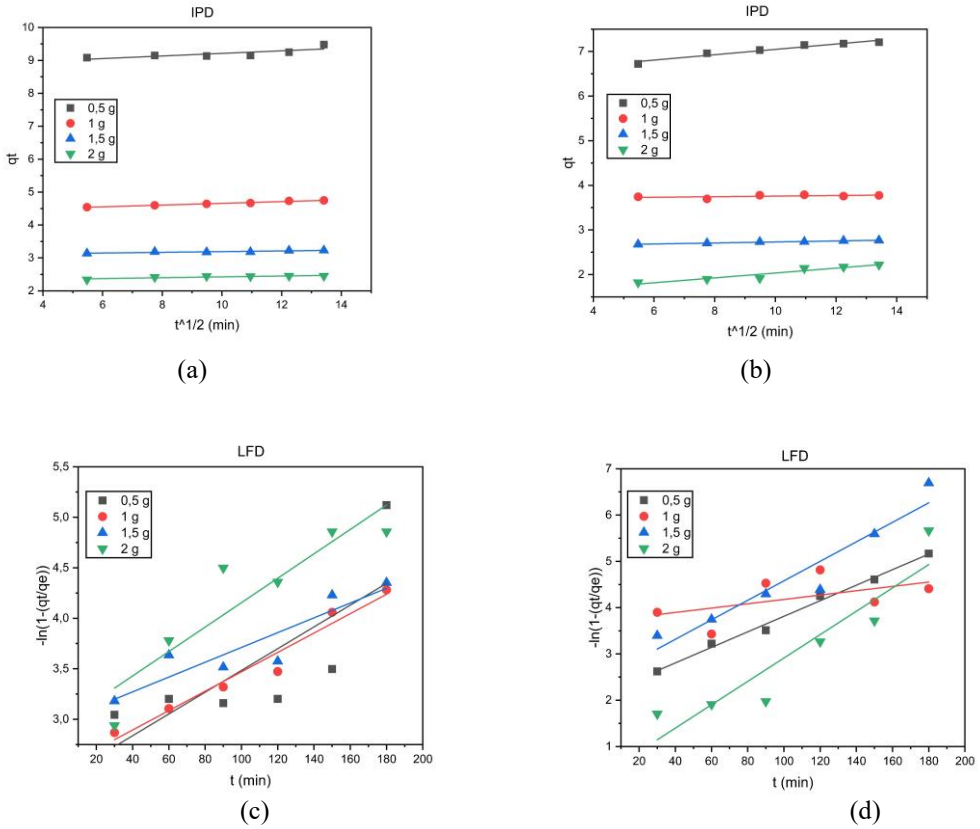

Figure 3 Linear regression of IPD kinetics model (a) Ni, (b) Co, and LFD kinetics models (c) Ni, (d) Co

4. CONCLUSIONS

According to the research results obtained, it reveals that the performance of ZT adsorbent on Ni will be higher when compared to Co, which is caused by numerous variables, including the smaller atomic radius of Ni compared to Co, more negative hydration energy, and more stability in solution. Furthermore, Ni also has a stronger affinity, so it will be more easily absorbed. All of the adsorption stages of Ni and Co follow the PSO kinetic model with a correlation coefficient value (R^2) > 0.99 so that the adsorption process of Ni and Co by ZT adsorbent is dominated by chemical interactions through ion exchange and the formation of coordination covalent bonds with active sites on the adsorbent surface. Furthermore, the correlation coefficients (R^2) for the IPD kinetic model ranged from 0.31 to 0.98, while those for the LFD kinetic model ranged from 0.28 to 0.99.

REFERENCES

[1] Y. Liu, G. Wang, Q. Luo, X. Li, and Z. Wang, "The thermodynamics and kinetics for the removal of copper and nickel ions by the zeolite Y synthesized from fly ash," *Mater. Res. Express*, vol. 6, no. 2, p. 25001, 2019, doi: 10.1088/2053-1591/aaea41.

[2] H. Leinonen, J. Lehto, and A. Mäkelä, "Purification of nickel and zinc from waste waters of metal-plating plants by ion exchange," *React. Polym.*, vol. 23, no. 2, pp. 221–228, 1994, doi: https://doi.org/10.1016/0923-1137(94)90024-8.

[3] A. A. Kamal, A. K. Mahmood, and S. Duja, "Remediation of clayey soil contaminated with nickel nitrate using enhanced Electro-Kinetics process and study the geotechnical properties of the remediated soil samples," *Mater. Today Proc.*, vol. 42, pp. 2516–2520, 2021, doi:

https://doi.org/10.1016/j.matpr.2020.12.572.

[4] H. Świnder and P. Lejwoda, "Obtaining Nickel Concentrates from Sludge Produced in the Process of Electrochemical Metal Surface Treatment," *Water, Air, Soil Pollut.*, vol. 232, no. 12, p. 505, 2021, doi: 10.1007/s11270-021-05456-x.

[5] G. Bartzas, P. E. Tsakiridis, and K. Komnitsas, "Nickel industry: Heavy metal(loid)s contamination - sources, environmental impacts and recent advances on waste valorization," *Curr. Opin. Environ. Sci. Heal.*, vol. 21, p. 100253, 2021, doi: https://doi.org/10.1016/j.coesh.2021.100253.

[6] K. Czarnek, S. Terpiłowska, and A. K. Siwicki, "Selected aspects of the action of cobalt ions in the human body.," *Cent. J. Immunol.*, vol. 40, no. 2, pp. 236–242, 2015, doi: 10.5114/ceji.2015.52837.

[7] E. Patel, C. Lynch, V. Ruff, and M. Reynolds, "Co-exposure to nickel and cobalt chloride enhances cytotoxicity and oxidative stress in human lung epithelial cells.," *Toxicol. Appl. Pharmacol.*, vol. 258, no. 3, pp. 367–375, Feb. 2012, doi: 10.1016/j.taap.2011.11.019.

[8] K. Sule, J. Umbsaar, and E. J. Prenner, "Mechanisms of Co, Ni, and Mn toxicity: From exposure and homeostasis to their interactions with and impact on lipids and biomembranes," *Biochim. Biophys. Acta - Biomembr.*, vol. 1862, no. 8, p. 183250, 2020, doi: https://doi.org/10.1016/j.bbamem.2020.183250.

[9] J. Parades-Aguilar *et al.*, "Removal of nickel(II) from wastewater using a zeolite-packed anaerobic bioreactor: Bacterial diversity and community structure shifts," *J. Environ. Manage.*, vol. 279, p. 111558, 2021, doi: https://doi.org/10.1016/j.jenvman.2020.111558.

[10] W. M. Saod, N. J. Alaallah, E. A. Abdulkareem, N. N. Hilal, and M. I. AlBiajawi, "Study of effective removal of nickel and cobalt from aqueous solutions by FeO@mSiO2 nanocomposite," *Results Chem.*, vol. 13, p. 101992, 2025, doi: https://doi.org/10.1016/j.rechem.2024.101992.

[11] E. Noman *et al.*, "Sustainable approaches for nickel removal from wastewater using bacterial biomass and nanocomposite adsorbents: A review," *Chemosphere*, vol. 291, p. 132862, 2022, doi: https://doi.org/10.1016/j.chemosphere.2021.132862.

[12] Z. Kazemi, F. Marahel, T. Hamoule, and B. M. Goodajdar, "Removal of Ni(II) and Co(II) ions from aqueous solutions utilizing Origanum majorana-capped silver nanoparticles," *Desalin. Water Treat.*, vol. 213, pp. 381–394, 2021, doi: https://doi.org/10.5004/dwt.2021.26727.

[13] Renu, M. Agarwal, and K. Singh, "Heavy metal removal from wastewater using various adsorbents: a review," *J. Water Reuse Desalin.*, vol. 7, no. 4, pp. 387–419, Nov. 2016, doi: 10.2166/wrd.2016.104.

[14] Y. Fei and Y. H. Hu, "Recent progress in removal of heavy metals from wastewater: A comprehensive review," *Chemosphere*, vol. 335, p. 139077, 2023, doi: https://doi.org/10.1016/j.chemosphere.2023.139077.

[15] N. A. A. Qasem, R. H. Mohammed, and D. U. Lawal, "Removal of heavy metal ions from wastewater: a comprehensive and critical review," *npj Clean Water*, vol. 4, no. 1, 2021, doi: 10.1038/s41545-021-00127-0.

[16] M. Sultana, M. H. Rownok, M. Sabrin, M. H. Rahaman, and S. M. N. Alam, "A review on experimental chemically modified activated carbon to enhance dye and heavy metals adsorption," *Clean. Eng. Technol.*, vol. 6, p. 100382, 2022, doi: 10.1016/j.clet.2021.100382.

[17] D. S. Patil, S. M. Chavan, and J. U. K. Oubagaranadin, "A review of technologies for manganese removal from wastewaters," *J. Environ. Chem. Eng.*, vol. 4, no. 1, pp. 468–487, 2016, doi: 10.1016/j.jece.2015.11.028.

[18] A. K. Kushwaha, N. Gupta, and M. C. Chattopadhyaya, "Dynamics of adsorption of Ni(II), Co(II) and Cu(II) from aqueous solution onto newly synthesized poly[N-(4-[4-(aminophenyl)methylphenylmethacrylamide])]," *Arab. J. Chem.*, vol. 10, pp. S1645–S1653, 2017, doi: 10.1016/j.arabjc.2013.06.007.

[19] M. Mambetova, K. Dossumov, M. Baikhamurova, and G. Yergaziyeva, "Sorbents Based on Natural Zeolites for Carbon Dioxide Capture and Removal of Heavy Metals from Wastewater: Current Progress and Future Opportunities," *Processes*, vol. 12, no. 10, 2024, doi: 10.3390/pr12102071.

[20] M. A. Afandy and F. D. I. Sawali, "Effect Of Concentration On Kinetics And Thermodynamics Parameter In The Cu (II) Removal By Activated Zeolite," *J. Integr. Proses*, vol. 13, no. 2, pp. 174–183, 2024.

[21] M. Irannajad and H. K. Haghighi, "Removal of Co2+, Ni2+, and Pb2+ by manganese oxide-coated zeolite: Equilibrium, thermodynamics, and kinetics studies," *Clays Clay Miner.*, vol. 65, no. 1, pp. 52–62, 2017, doi: 10.1346/CCMN.2016.064049.

[22] D. W. Astuti, Mudasir, and N. H. Aprilita, "Preparation and characterization adsorbent based on zeolite from Klaten, Central Java, Indonesia," *J. Phys. Conf. Ser.*, vol. 1156, no. 1, pp. 0–6, 2019, doi: 10.1088/1742-6596/1156/1/012002.

[23] M. Sirotiak, B. Alica, and L. Blinová, "Uv-Vis Spectrophotometric Determinations of Selected Elements in Modelled Aqueous Solutions," *J. Environ. Prot. Safety, Educ. Manag.*, vol. 2, no. 3, pp. 75–87, 2014.

[24] F. A. Rasheed, M. Sillanpää, and M. Moradi, "Cobalt adsorption by Ca(OH)2 Modified quartz rock particles adsorbent: Equilibrium isotherm, kinetics, and thermodynamic studies," *Desalin. Water Treat.*, vol. 319, no. June, p. 100477, 2024, doi: 10.1016/j.dwt.2024.100477.

[25] J. L. Diaz De Tuesta *et al.*, "Performance and modeling of Ni(II) adsorption from low concentrated wastewater on carbon microspheres prepared from tangerine peels by FeCl3-assisted hydrothermal carbonization," *J. Environ. Chem. Eng.*, vol. 10, no. 5, 2022, doi: 10.1016/j.jece.2022.108143.

[26] D. W. Breck, *Zeolite Molecular Sieves: Structure, Chemistry, and Use*. Wiley, 1973. [Online]. Available: https://books.google.co.id/books?id=aY0vAQAAIAAJ

[27] Y. Marcus, "Thermodynamics of Solvation of Ions," vol. 87, no. 18, pp. 2995–2999, 1991.

[28] S. Wang and Y. Peng, "Natural zeolites as effective adsorbents in water and wastewater treatment," vol. 156, pp. 11–24, 2010, doi: 10.1016/j.cej.2009.10.029.

[29] S. S. S. Hosseini, A. Khosravi, H. Tavakoli, M. Esmhosseini, and S. Khezri, "Natural zeolite for nickel ions removal from aqueous solutions: optimization and modeling using response surface methodology based on central composite design," *Desalin. Water Treat.*, vol. 57, no. 36, pp. 16898–16906, 2016, doi: 10.1080/19443994.2015.1082508.

[30] F. Bahmanzadegan and A. Ghaemi, "A comprehensive review on novel zeolite-based adsorbents for environmental pollutant," *J. Hazard. Mater. Adv.*, vol. 17, no. December 2024, p. 100617, 2025, doi: 10.1016/j.hazadv.2025.100617.

[31] Darmansyah, S. B. Ginting, D. A. Iryani, R. P. Sari, and D. Supriyadi, " Characterization of Modified Lampung Natural Zeolite with Cetyl Trimethyl Ammonium Bromide (CTAB) for Adsorption Industrial Tapioca Wastewater ," *Proc. Int. Conf. Sustain. Biomass (ICSB 2019)*, vol. 202, no. Icsb 2019, pp. 230–235, 2021, doi: 10.2991/aer.k.210603.041.

[32] B. B. Ferri *et al.*, "Natural zeolite as adsorbent for metformin removal from aqueous solutions: Adsorption and regeneration properties," *Desalin. Water Treat.*, vol. 320, no. May, p. 100602, 2024, doi: 10.1016/j.dwt.2024.100602.

[33] E. Heraldy, H. SW, and S. Sulistiyono, "Characterization and Activation of Natural Zeolit From Ponorogo," *Indones. J. Chem.*, vol. 3, no. 2, pp. 91–97, 2010, doi: 10.22146/ijc.21891.